RUHR-UNIVERSITÄT BOCHUM

RUB

CR propagation and magnetic fields in galactic halos: observational evidence of CR driven galactic winds ？

Ralf-Jürgen Dettmar, Ruhr-University Bochum

with V. Heesen, B. Adebahr, R. Beck, M. Krause,Y. Stein,
M. Wezgowiec, A. Miskolczi, George Heald and the
LOFAR MKSP & CHANGES teams

What we can measure: synchrotron emission from CR electrons

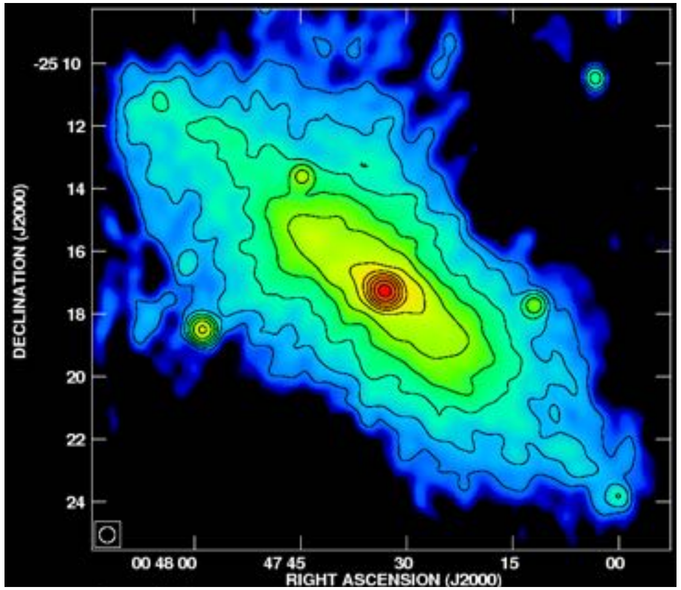

NGC 253 radiocontinuum study at 3, 6, 20, 90 cm

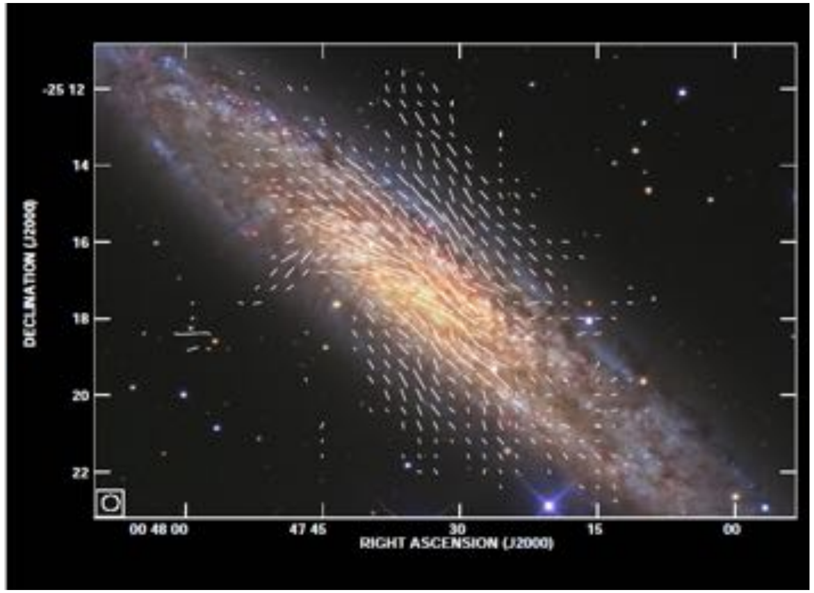

(Heesen, Krause, Beck, Dettmar 2009 A&A)

Polarized emission (and angles):

$I \propto \int n_{CR} B_{\perp}^{1+\alpha} dl$

Faraday rotation measures of the diffuse polarized emission:

$RM \propto \int n_e B_{\parallel} dl$

Cosmic ray-driven winds

LAUNCHING COSMIC-RAY-DRIVEN OUTFLOWS FROM THE MAGNETIZED INTERSTELLAR MEDIUM

Philipp Girichidis[1], Thorsten Naab[1], Stefanie Walch[2], Michał Hanasz[3], Mordecai-Mark Mac Low[4,5], Jeremiah P. Ostriker[6], Andrea Gatto[1], Thomas Peters[1], Richard Wünsch[7], Simon C. O. Glover[5], Ralf S. Klessen[5], Paul C. Clark[8], and Christian Baczynski[5] —Hide full author list

Published 2016 January 6 •
The Astrophysical Journal Letters, Volume 816, Number 2

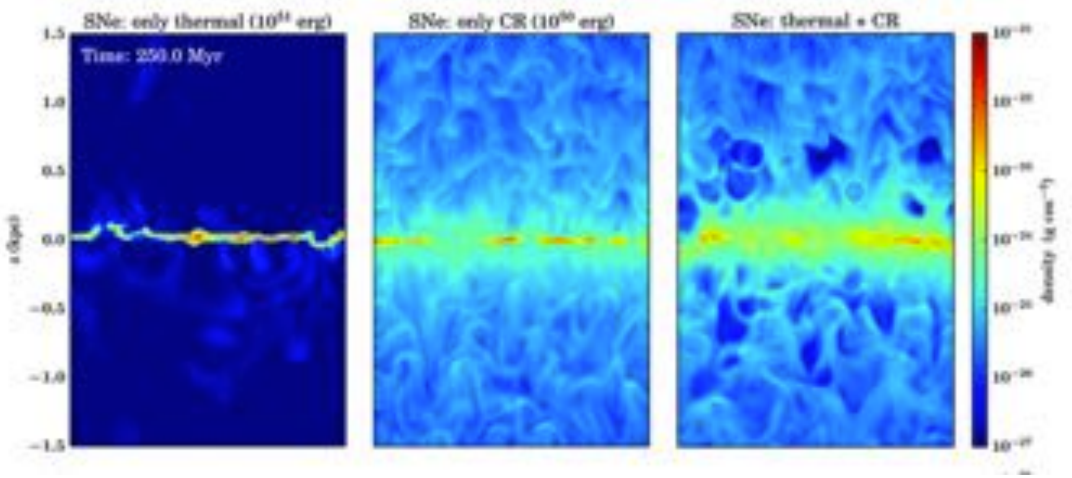

Salem & Bryan (2014)

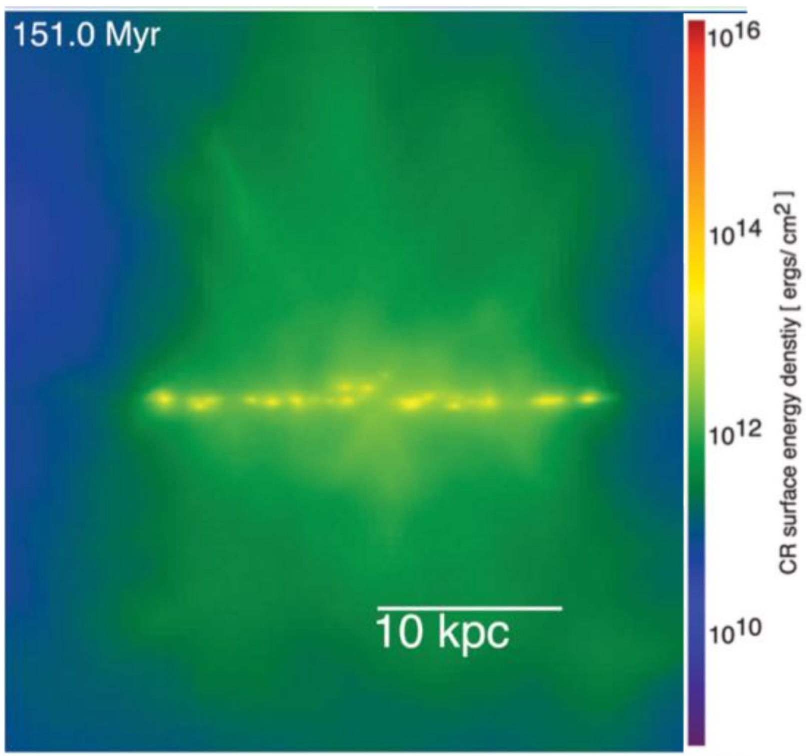

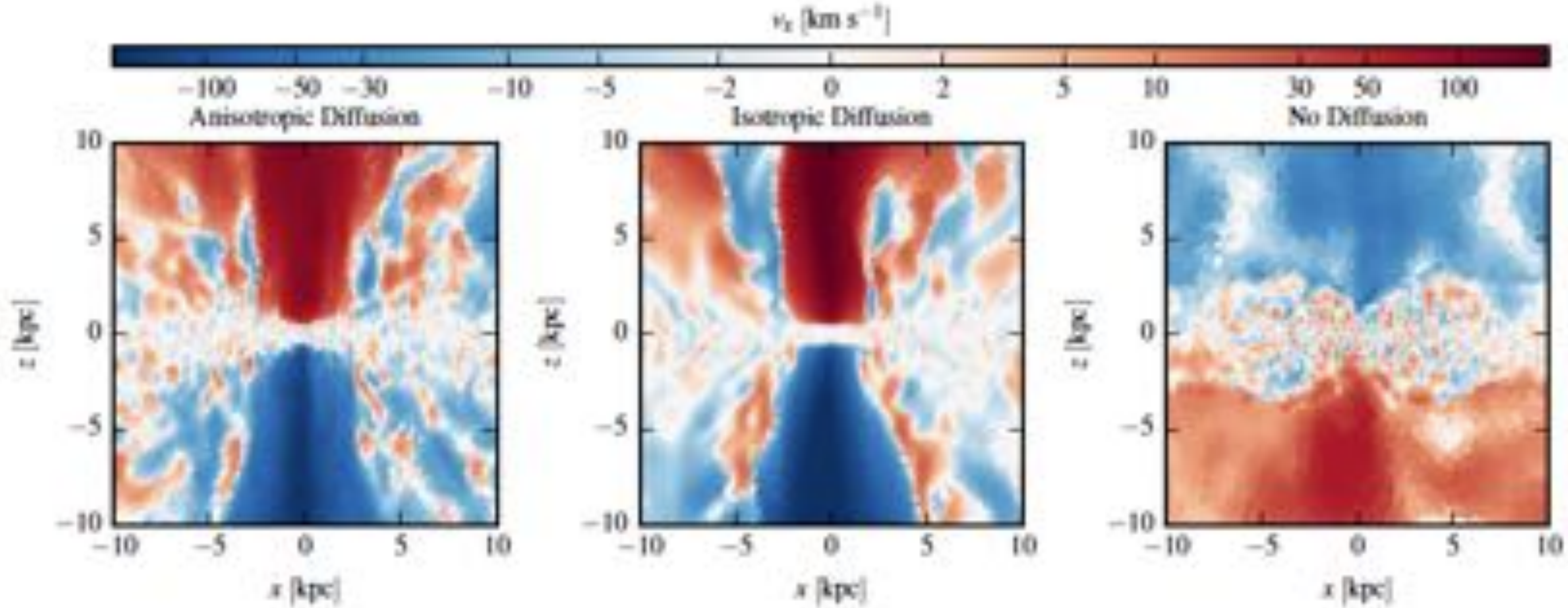

Pakmor, Pfrommer, Simpson, Springel (2016)

Recent progress based on:

- new facilities — LOFAR, upgraded JVLA, GMRT, ATCA, WSRT
- new methods — RM synthesis, QU fitting
- better auxiliary data — dust emission & other SF tracer

new facilities: example LOFAR

LOFAR HBA at Jülich (FZ Jülich- RU Bochum)

new facilities: example LOFAR: LoTTS survey

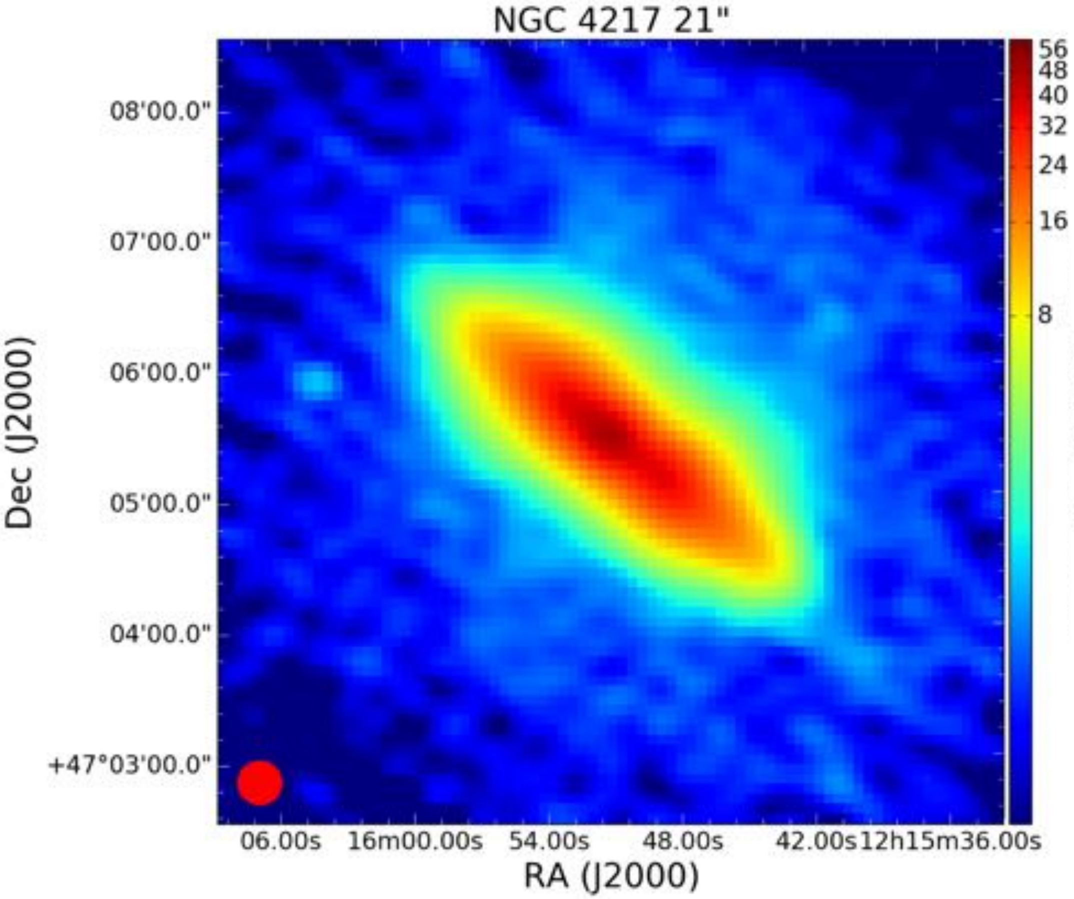

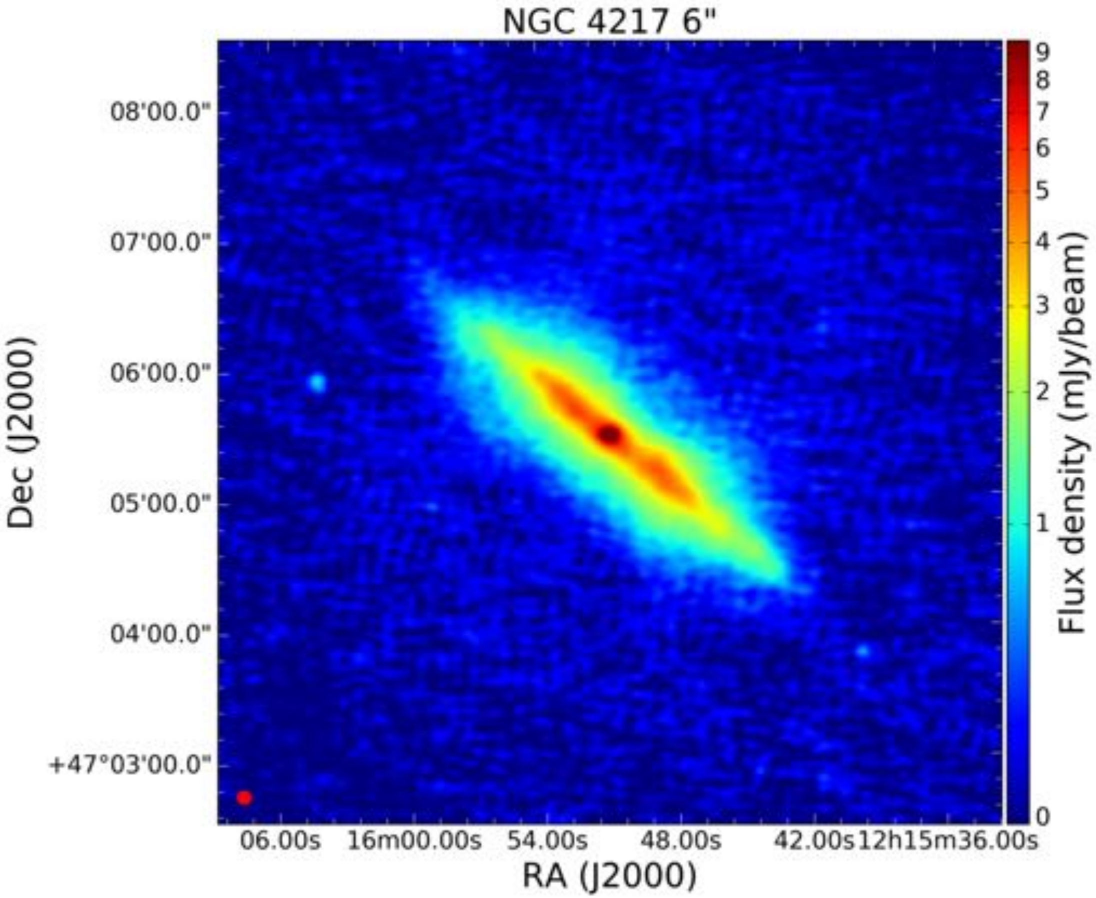

~0.1 mJy rms noise, 0.46Jy total flux (A. Miskolczi)

new methods: e.g. RM synthesis

- Better calibration of interferometric data with strong off-axis sources (Peeling, Oosterloo, de Bruyn)
- Single-dish cleaning technique for high-dynamic range single dish imaging (strong sources observed with Effelsberg)
- Use of multichannel receivers for calibration and
- Rotation Measure-synthesis (demonstrated with WSRT data), f Faraday depth

$$P(\lambda^2) = \int_{-\infty}^{+\infty} pI e^{2i[\chi_0 + \phi\lambda^2]} \mathrm{d}\phi$$

$$P(\lambda^2) = \int_{-\infty}^{+\infty} F(\phi) e^{2i\phi\lambda^2} \mathrm{d}\phi,$$

F(f) Faraday dispersion function

(G. Heald)

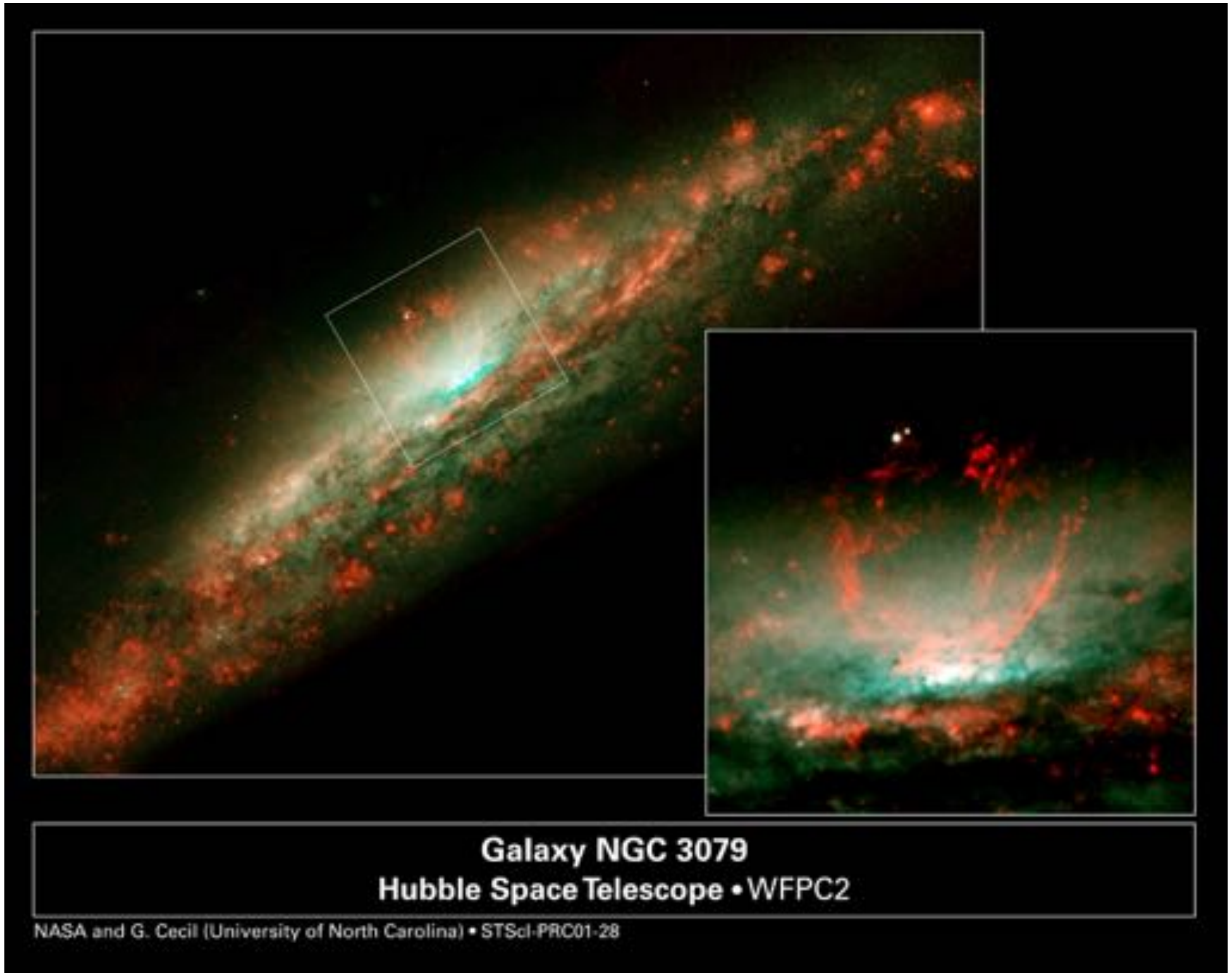
Galaxy NGC 3079
Hubble Space Telescope • WFPC2
NASA and G. Cecil (University of North Carolina) • STScI-PRC01-28

Rotation Measure Synthesis

WSRT observations of NGC3079

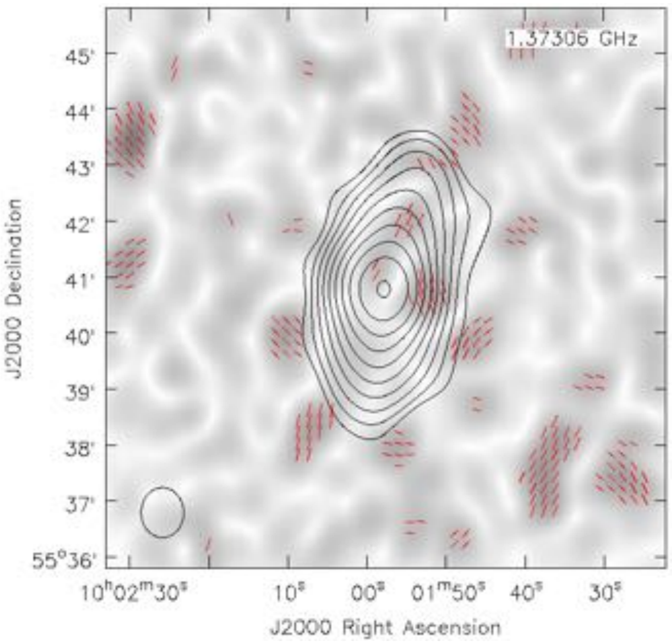

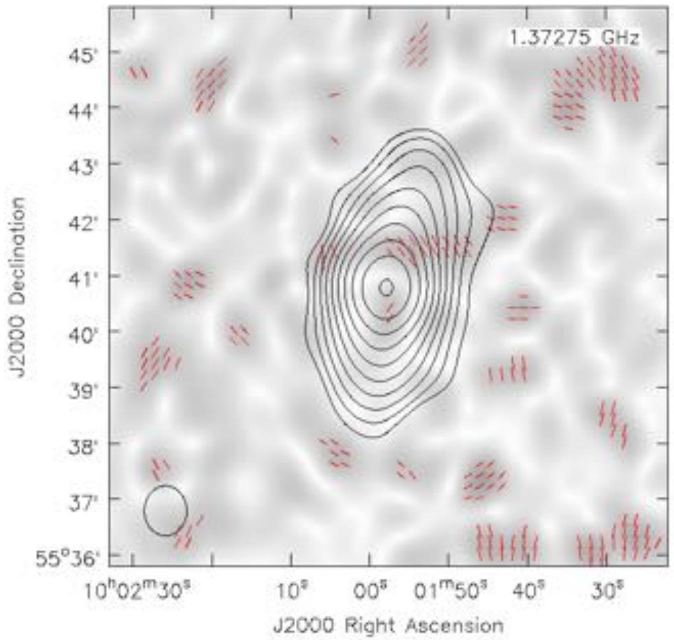

Carlos Sotomayor (PhD Bochum 2014)

N3079 (WRST)

H_alpha + HST insert

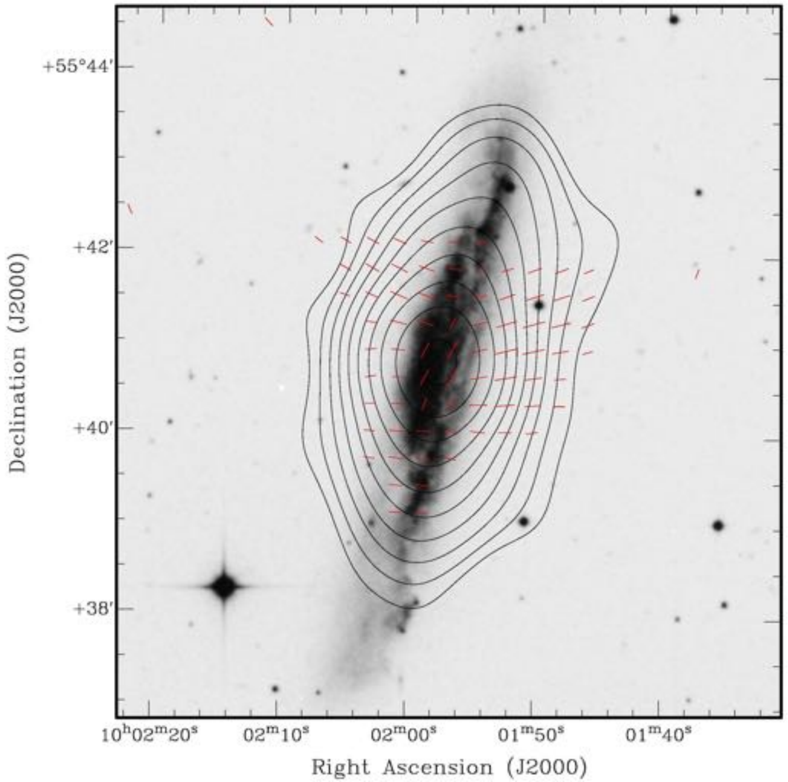

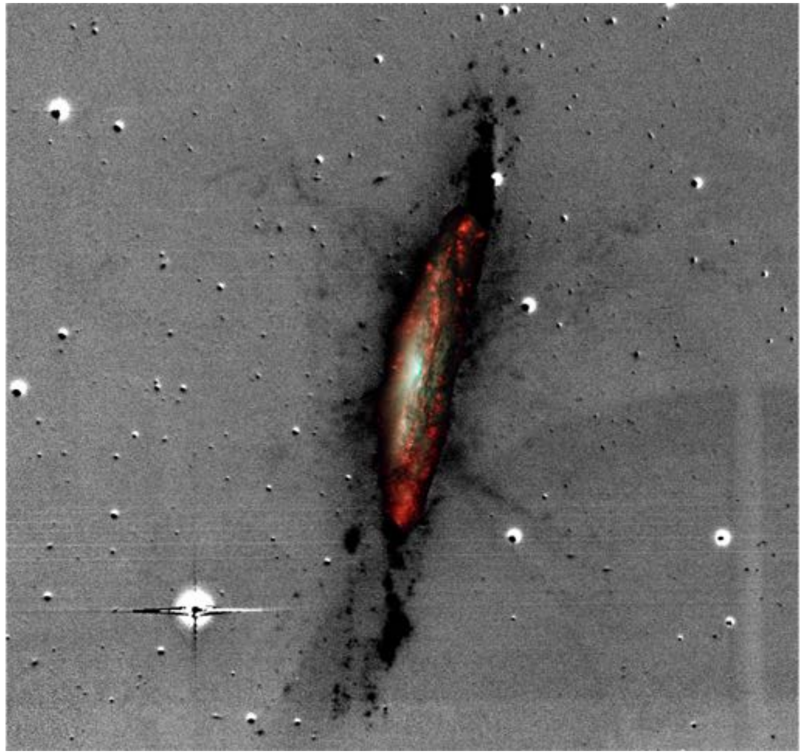

Carlos Sotomayor (PhD Bochum 2014)

Bomans, Miskolczi (in prep.)

X-ray emission
Starburst galaxy NGC 3079

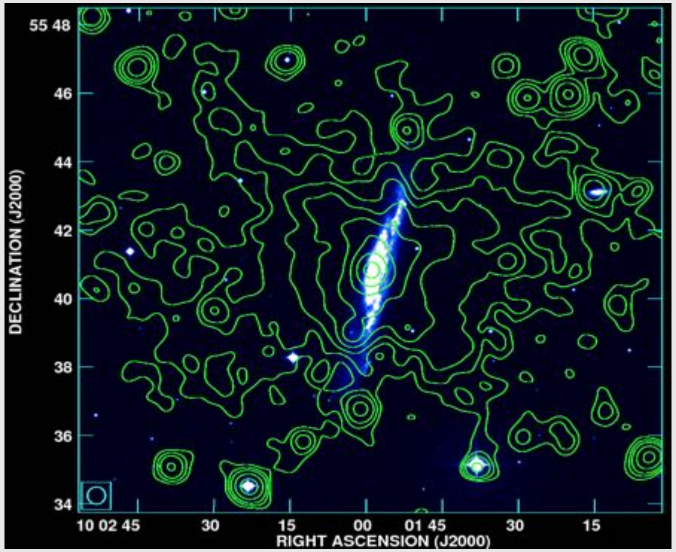

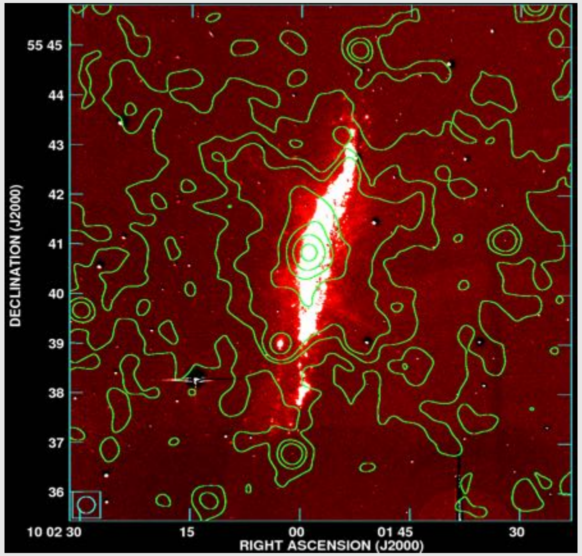

NGC 3079 soft X-ray image based on XMM-Newton archives (M. Wezgowiec).

(18 ks of clean pn data)

better auxiliary data:
thermal/non-thermal separation

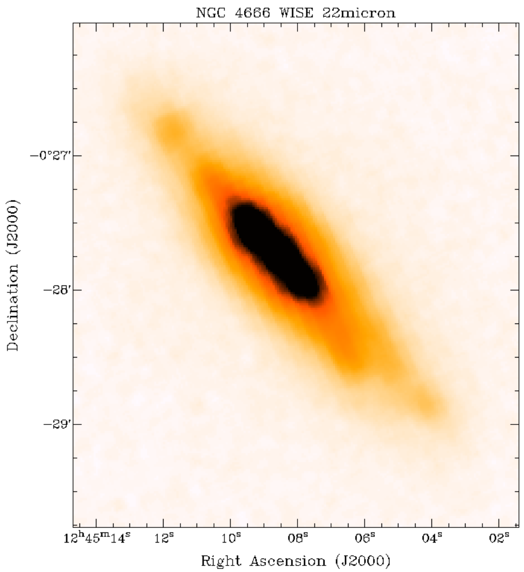

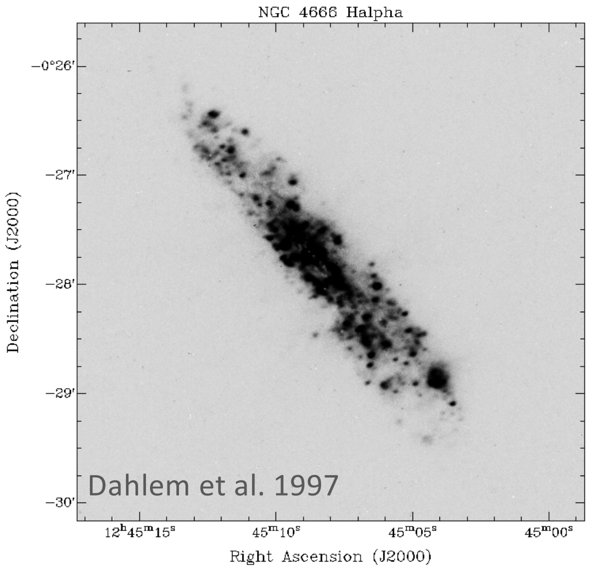

Dust corrected Hα image as thermal emission:

- WISE (22 μm) and Hα (in erg/s)
- Smoothing, regridding
- Calculating thermal Flux based on Calzetti et al. 2007

$F_{thermal} = C \; (L_{H\alpha} + 0.04\, L_{WISE})$

C. Vargas+ 2018. CHANG-ES X: Spatially Resolved Separation of Thermal Contribution from Radio Continuum Emission in Edge-on Galaxies

“clean non-thermal emission”: 1D Modelling of CR–Transport

N(E, z): Cosmic Ray Electron number (column) density

Advection: $$\frac{\partial N(E,z)}{\partial z} = \frac{1}{V}\left\{\frac{\partial}{\partial E}\left[b(E)N(E,z)\right]\right\}$$

Diffusion: $$\frac{\partial^2 N(E,z)}{\partial z^2} = \frac{1}{D}\left\{\frac{\partial}{\partial E}\left[b(E)N(E,z)\right]\right\}$$

CRe losses: $$-\left(\frac{\mathrm{d}E}{\mathrm{d}t}\right) = b(E) = \frac{4}{3}\sigma_{\mathrm{T}}c\left(\frac{E}{m_{\mathrm{e}}c^2}\right)^2(U_{\mathrm{rad}} + U_{\mathrm{B}})$$

iC losses → U_{rad}

synchrotron radiation → U_{B}

CRE transport: SPINNAKER (V. Heesen)

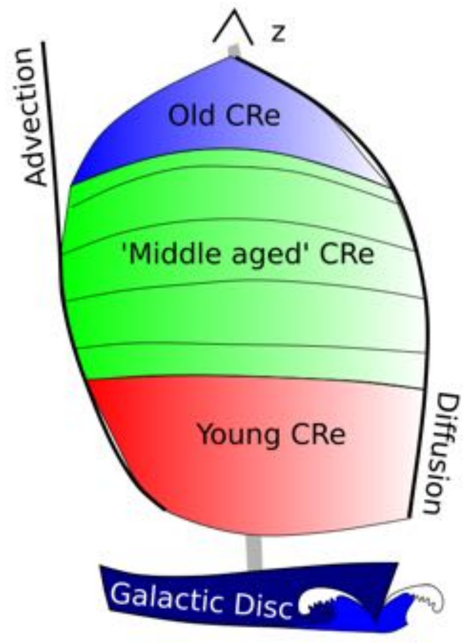

- **Sp**ectral **In**dex **N**umerical **A**nalysis of **K**(c)osmic-ray **E**lectron **R**adio-emission
- www.github.com/vheesen/Spinnaker

Advection models

h_B = 4 kpc h_B = 8 kpc h_B = 1e4 kpc

N(E,z)

$I_{nt}(z)$

α_{nt}

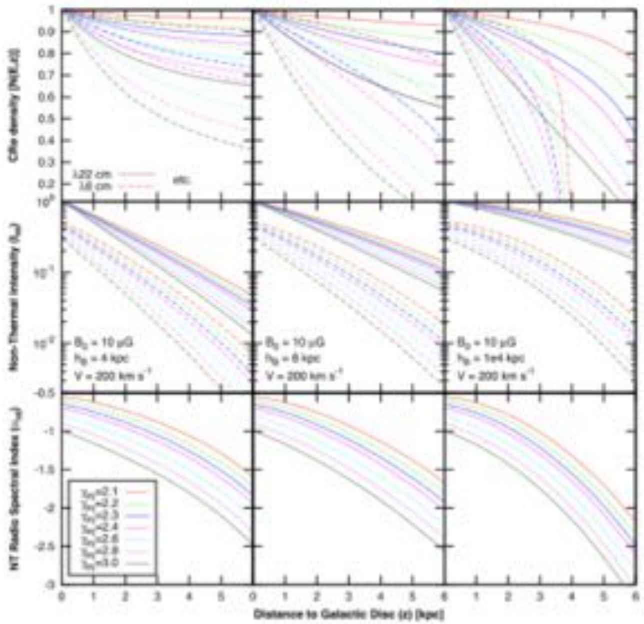

Diffusion models

h_B = 4 kpc h_B = 8 kpc h_B = 1e4 kpc

N(E,z)

$I_{nt}(z)$

α_{nt}

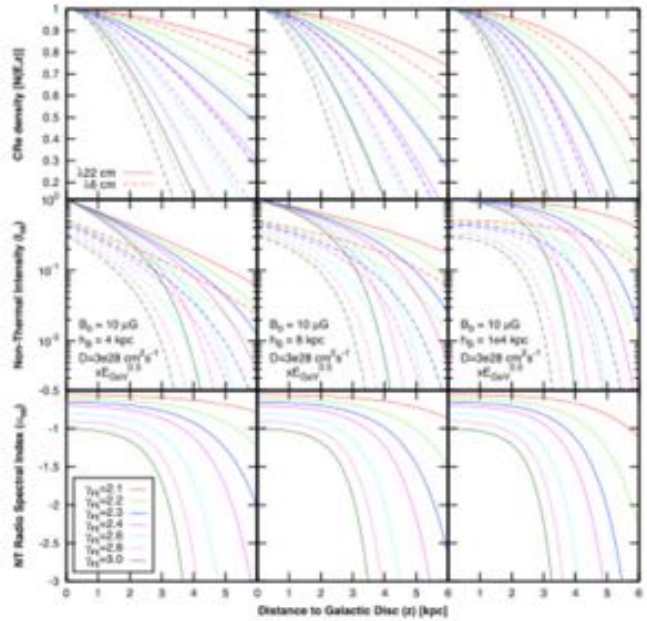

Example: ATCA Observations

22 + 6 cm, radio continuum polarimetry

~160 hr at 22 cm and ~60 hr at 6 cm each

rms: ~30 μJy/beam at 22 cm and ~15 μJy/beam at 6 cm

Cleaned with CASA multi-scale CLEAN

N7090

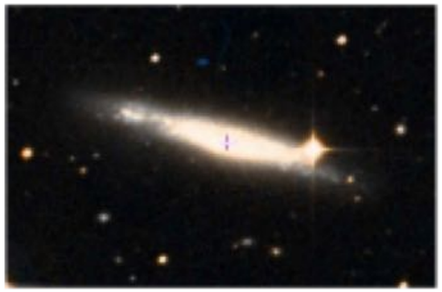

N7462

analysis of CR transport (ATCA 6&20cm)

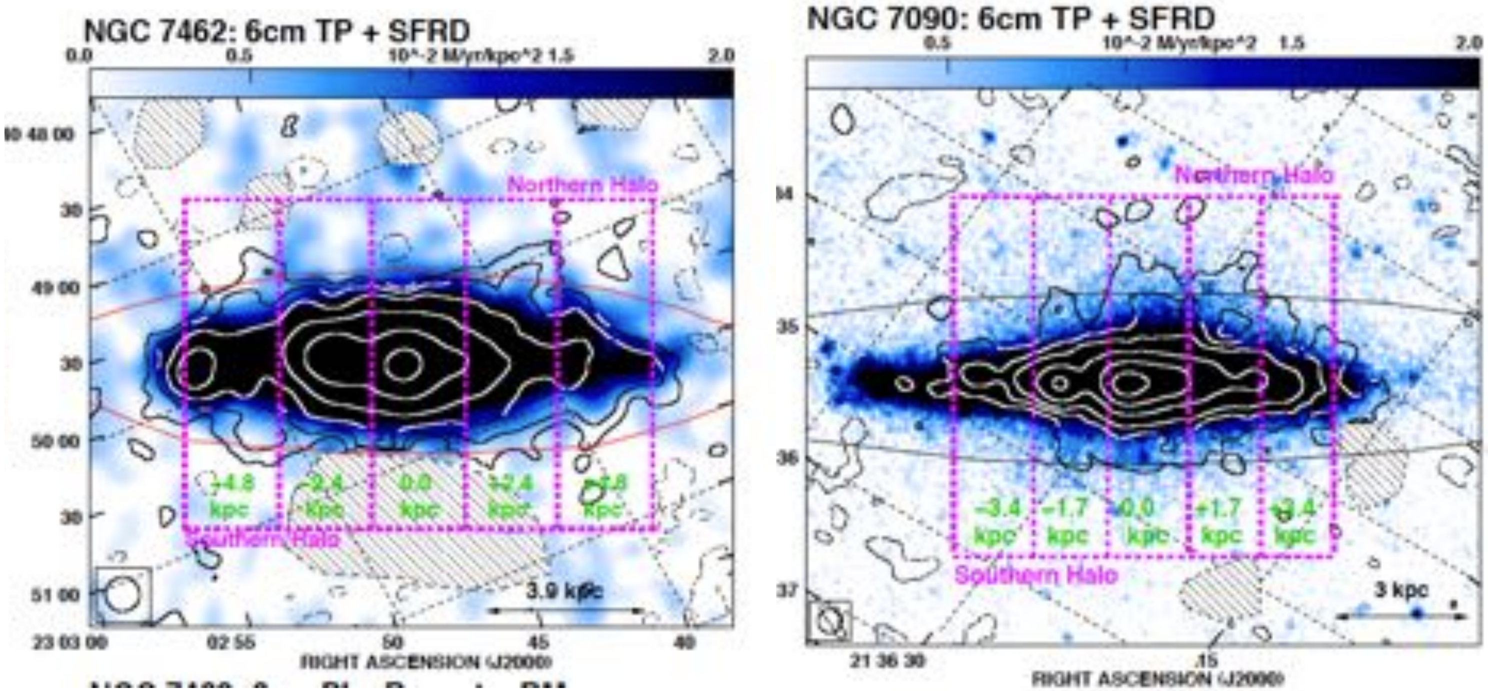

Heesen+ 2016 MNRAS 458, 332

Example: NGC 7090 advection model

Exponential intensity profiles
+ linear spectral index profiles

⇒ Advection dominated halo

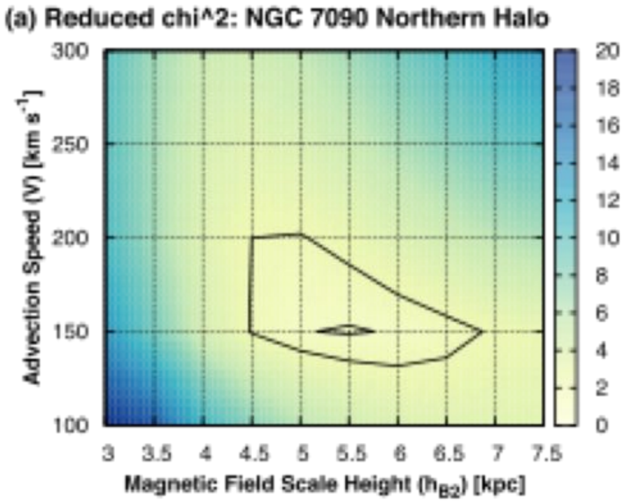

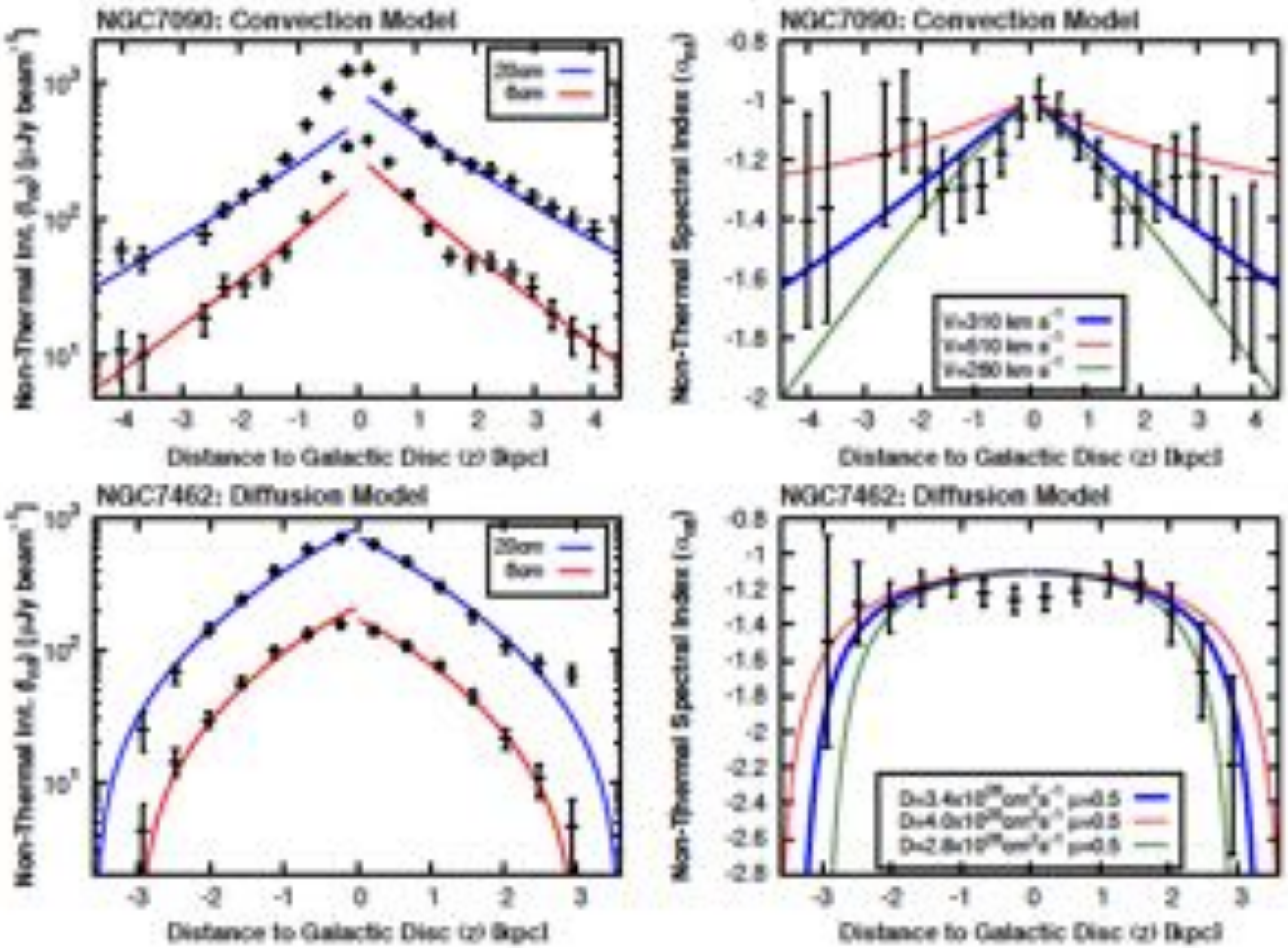
NGC7090: Convection Model
NGC7090: Convection Model
NGC7462: Diffusion Model
NGC7462: Diffusion Model
20cm
6cm
20cm
6cm
Non-Thermal Spectral Index
Distance to Galactic Disc (z) [kpc]

Table 2. Observation details for the galaxies presented in this paper.

Galaxy	Band[a]	ν[b] (GHz)	Telescope[c]	Configuration[d]	Project[e]	Time[f] (h)	Date[g]	Notes[h]	Reference[i]
NGC 55	*L*	1.37	ATCA	750D	C287	8.7	1993 Aug 1	Mosaic	17
...	...	...	...	375	C287	11.2	1995 Jan 12	...	...
...	...	...	...	750A	C287	11.1	1995 Oct 25	...	...
...	...	...	...	H75	C1341	5.0	2005 Jul 17	Mosaic	This work
...	...	...	...	EW352	C1341	9.4	2005 Oct 7	...	...
...	*C*	4.80	...	375	C287	3.6	1994 Mar 29	Mosaic	17
...	...	...	...	375	C287	10.2	1994 Mar 30	...	...
...	...	...	...	375	C287	7.8	1994 Mar 31	...	...
...	...	...	...	375	C287	12.5	1994 Nov 23	...	...
...	...	...	...	750A	C287	5.1	1995 Mar 1	...	...
...	...	...	...	375	C287	5.3	1995 Aug 16	...	...
...	...	...	...	375	C287	10.2	1995 Nov 24	...	...
...	...	4.67	...	EW352	C1974	7.6	2008 Nov 22	...	This work
...	...	...	...	EW364	C1974	9.9	2009 Feb 13	...	...
...	*C*	5.60	...	H168	C1974	7.6	2010 Mar 27	...	...
...	*C*	4.80	Parkes	single-dish	P697	16.0	2010 Oct 7	Merged	...
NGC 253	*L*	1.46	VLA	B+C+D	AC278	4.1	1990 Sep–1991 Mar	Mosaic	2
...	*C*	4.86	...	D	AH844	35.8	2004 Jul 4–24	Mosaic	10
...	...	4.85	Effelsberg	single-dish	N/A	N/A	1997	Merged	...
NGC 891	*L*	1.39	WSRT	Multiple	R02B	240	2002 Aug–Dec		13
...	*C*	4.86	VLA	D	AA94	11.2	1988 Aug 29		16
...	...	4.85	Effelsberg	single-dish	44–95	9.1	1996 Feb–Aug		6
NGC 3044	*L*	1.49	VLA	B	AI28	3.1	1986 Aug 1		This work
...	...	...	...	C	AI23	0.8	1985 Jul 25		11
...	...	...	...	D	AI31	1.1	1987 Apr 28/30		...
...	*C*	4.86	...	C	AB676	0.8	1993 Jun 13		4
...	...	...	...	D	AM573	1.1	1997 Nov 6		This work
...	...	...	...	D	AI31	1.0	1987 Apr 28		11
NGC 3079	*L*	1.66	VLA	B	BS44	1.0	1997 Mar 8		This work
...	...	1.41	...	CD	BS44	2.4	1997 Oct 2		...
...	...	1.43	...	C	AB740	1.3	1996 Feb 17		...
...	*C*	4.71	...	C	AC277	3.9	1990 Dec 9		3
...	...	4.86	...	D	AD177	2.5	1986 Jan 16		This work
NGC 3628	*L*	1.49	VLA	CD	AS300	4.3	1988 Mar 25		14
...	...	...	...	D	AS300	8.4	1987 Apr 7		...
...	*C*	4.86	...	D	AK243	7.7	1991 Mar 28		7
NGC 4565	*L*	1.49	VLA	B	AS326	3.8	1988 Jan 29		16
...	...	1.48	...	D	AS326	10.6	1988 Aug 28		...
...	*C*	4.86	...	D	AK424	3.4	1996 Sep 28		6
NGC 4631	*L*	1.37	WSRT	maxi-short	N/A	6.0	2003 Apr 3		1
...	*C*	4.86	VLA	D	AH369	12.1	1989 Nov 22/26	Mosaic	9
...	...	...	...	D	AD896	4.3	1999 Apr 14	Mosaic	12
...	...	4.85	Effelsberg	single-dish	55–94	6.3	1996 Feb–Aug	Merged	6
NGC 4666	*L*	1.43	VLA	CD	AD346	3.5	1994 Nov 20		5
...	...	1.49	...	D	AS199	0.2	1984 Aug 31		This work
...	*C*	4.86	...	D	AD326	12.5	1993 Dec 20/24		5
NGC 5775	*L*	1.49	VLA	B	AI0028	3.2	1986 Aug 1		8
...	...	1.48	...	B	AB492	1.2	1989 Aug 4		...
...	...	1.49	...	C	AH368	3.6	1990 Nov 19/24		...
...	...	...	...	D	AI31	1.9	1987 Apr 27/30		11
...	*X*	8.45	...	D	AD455	13.4	2001 Dec 14		15

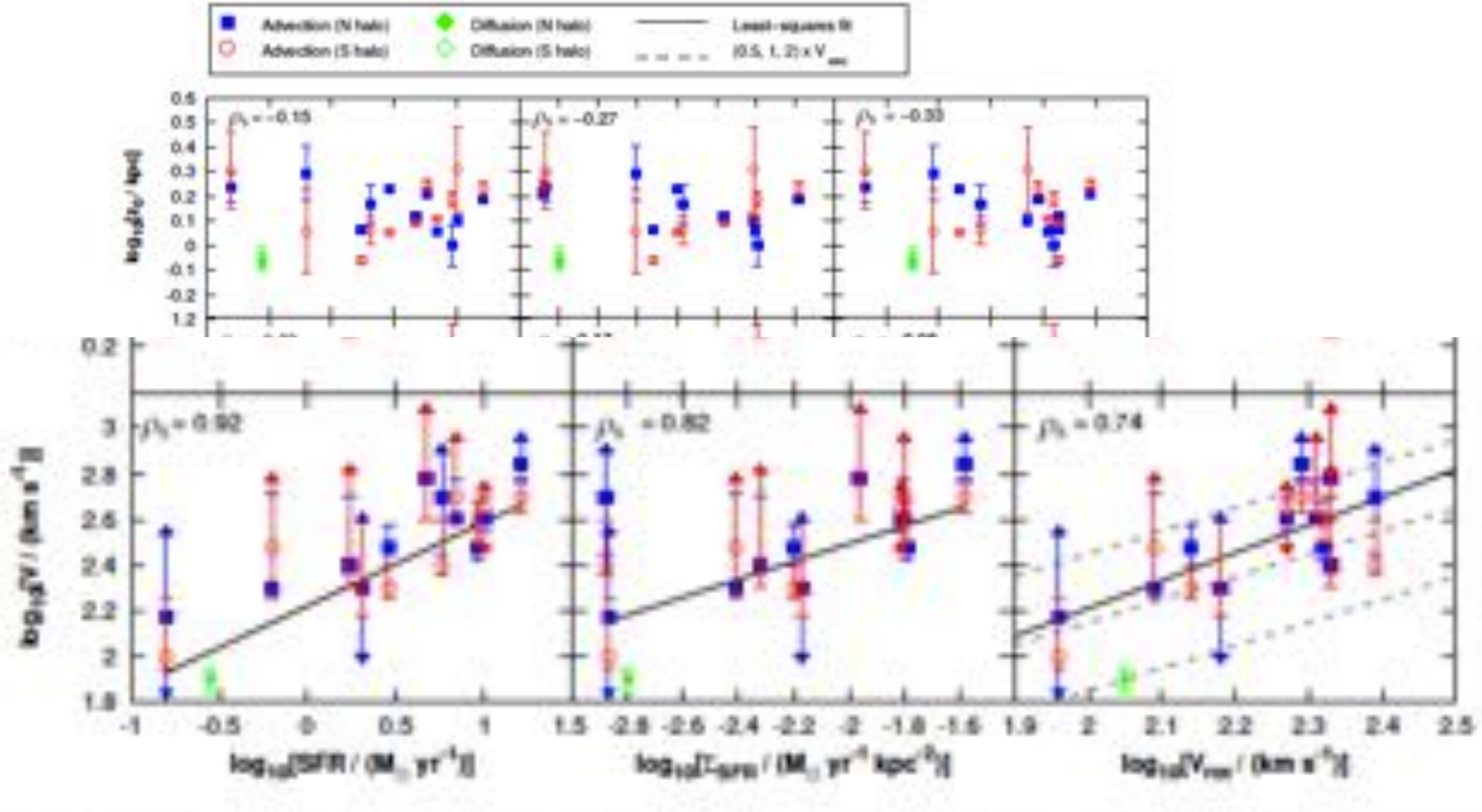

Figure 8. Parameter studies in log-log diagrams as function of SFR, SFR surface density (Σ_{SFR}) and rotation speed V_{rot}. *Top panels:* non-thermal intensity scale height (h_{syn}) at 5 GHz (8.5 GHz for NGC 5775) of the thick radio disc. *Middle panels:* magnetic field scale height (h_B) of the thick radio disc. *Bottom panels:* Advection speed (V), where solid lines show least-squares fits. In the bottom right panel the dashed lines show $(0.5, 1, 2)\times V_{esc}$. In each panel, we also present Spearman's rank correlation coefficient, ρ_s, which we derived from values that have both an upper and lower limits.

:

Heesen+ MNRAS 476,158 (2018)

CRAV (identical to NOCR but 10% of the SN energy in CR energy. The remaining 90% is added as thermal energy. The CR energy can advect with the gas

CRAD is identical to CRAV, but with *anisotropic* instead of isotropic CR diffusion (Pakmor et al. 2016a). The diffusion coefficient in this model is $\kappa = 10^{28}$ cm^2 s^{-1} parallel to the magnetic field and zero in all transverse directions.

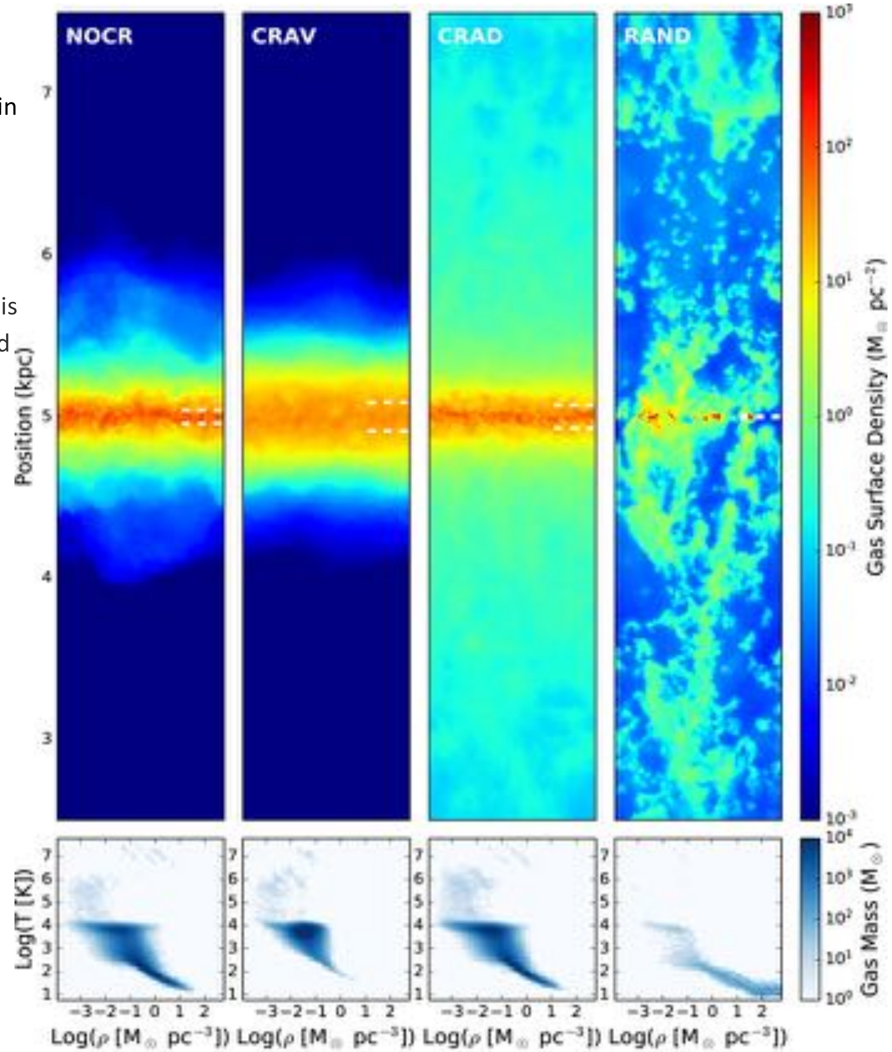

Christine M. Simpson et al. 2016 ApJL 827 L29

Making use of the JVLA

CHANGES:
Continuum HAlos in Nearby Galaxies
- an Evla Survey

PI: Judith Irwin, Kingston (ONT/CANADA)

35 edge-on galaxies

inclination > 75 deg
DEC > 25 deg
4 arcmin > D < 15 arcmin
flux > 23 mJy

+ a few well studied larger object

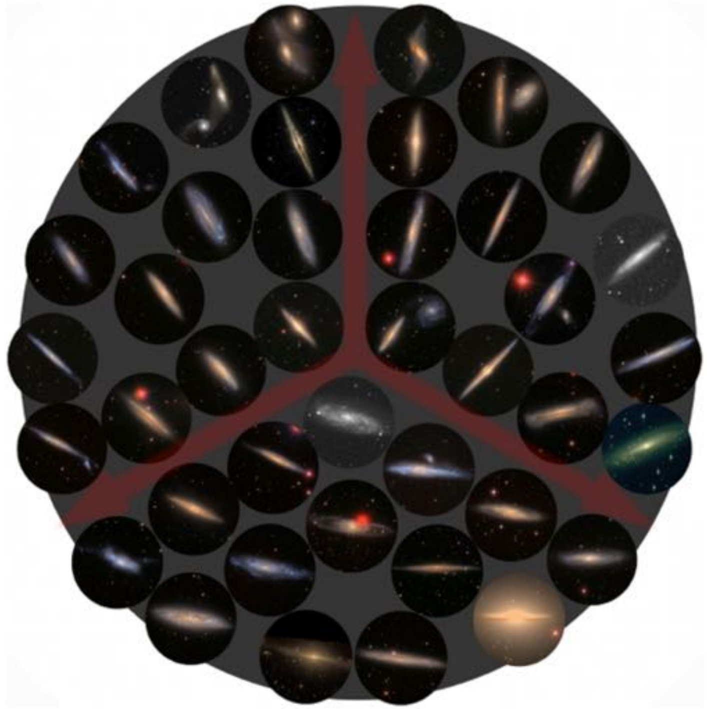

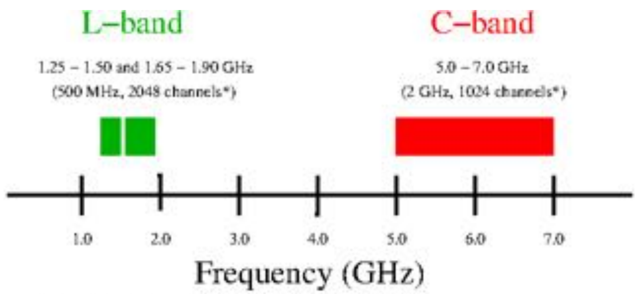

Large proposal 405 hours granted (RSRO)

Wiegert et al. AJ 150, 81 (2015) D-array C & L band

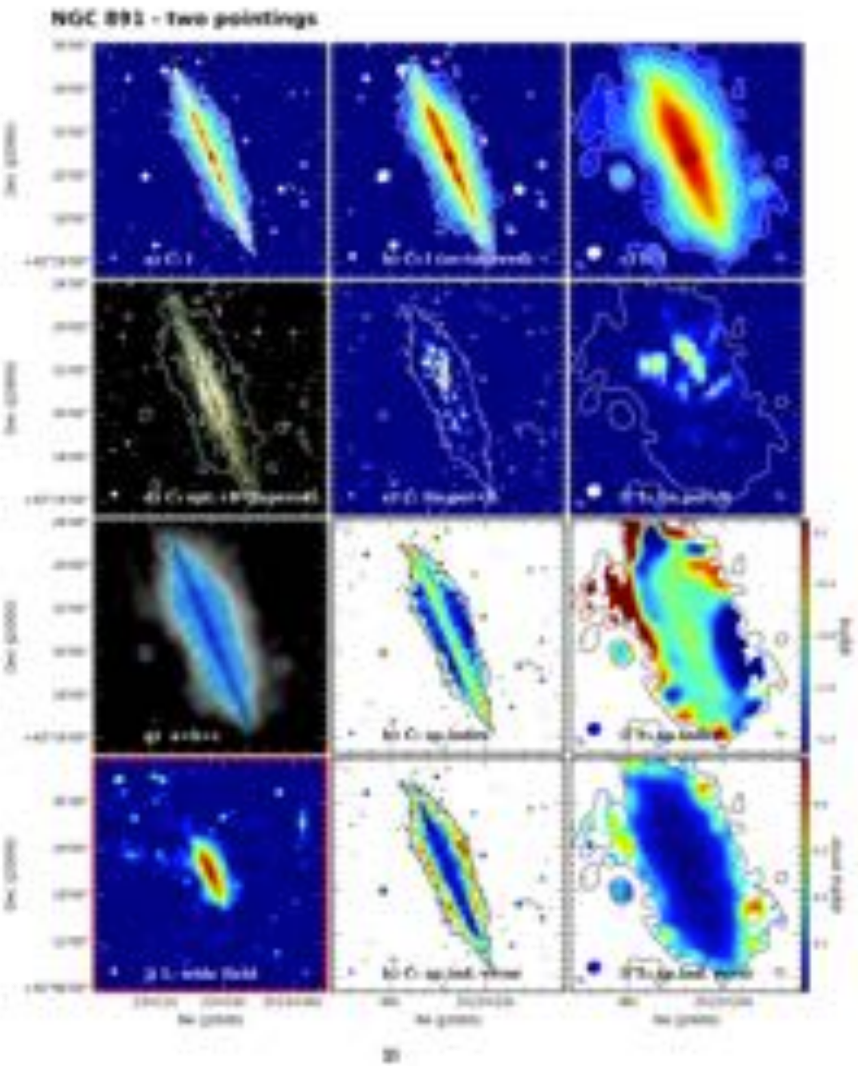

queensu.ca/changes

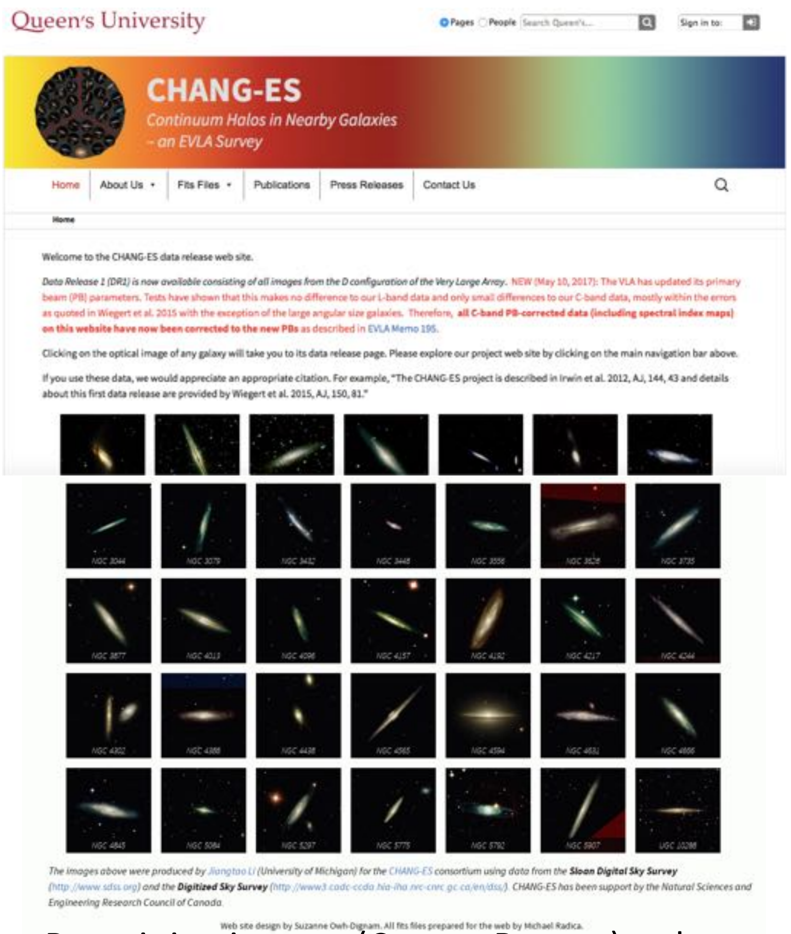

Remaining images (C array B array) to be released in 2019 sorted by SFR at common distance

„averaged“ radio continuum halo

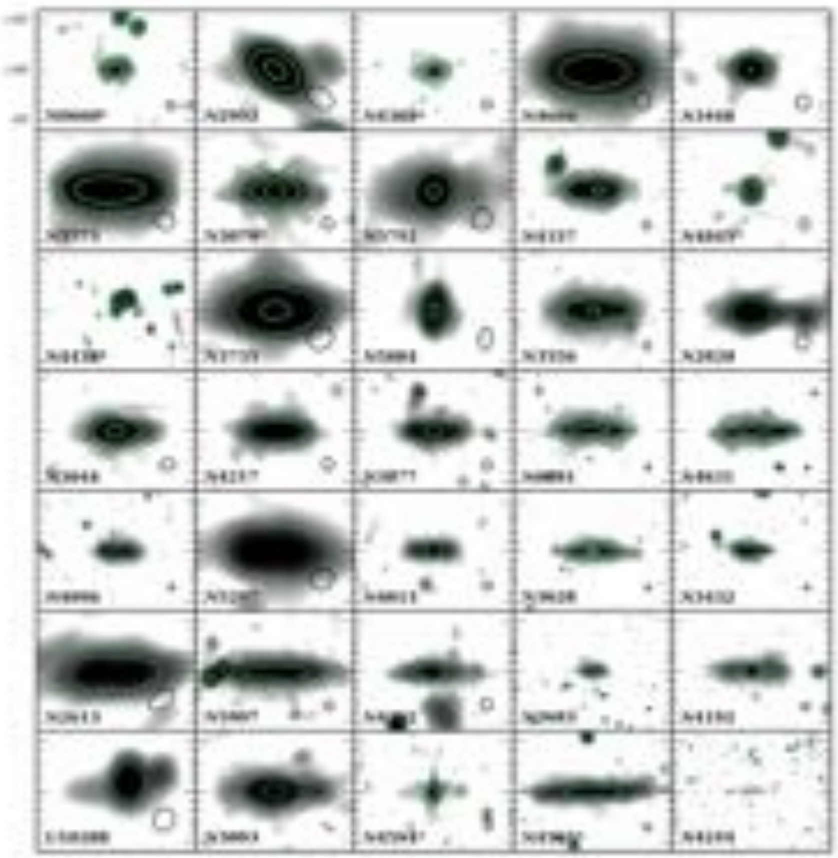

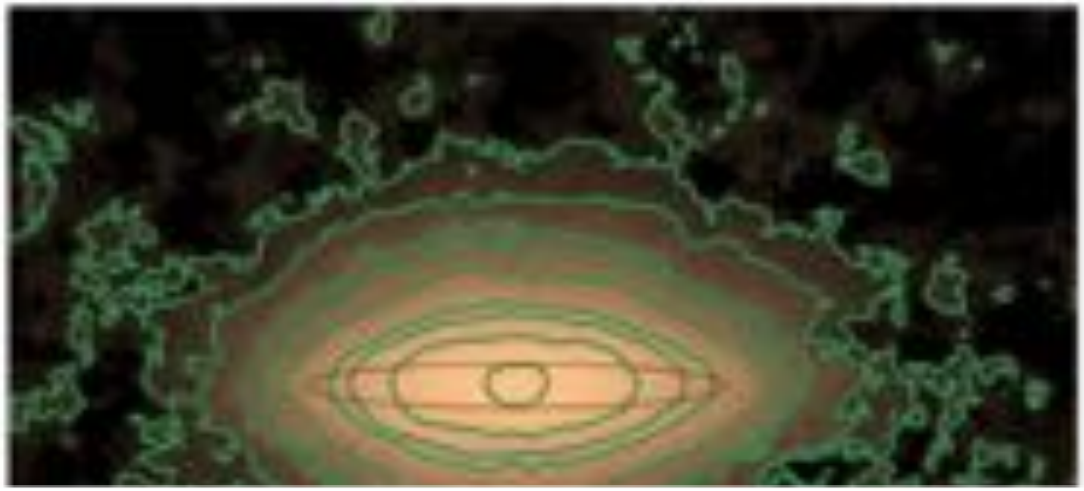

The Astrophysical Journal Letters, 799:L10 (6pp), 2015 January 20 doi:10.1088/2041-8205/799/1/L10

AXIAL RATIO OF EDGE-ON SPIRAL GALAXIES AS A TEST FOR BRIGHT RADIO HALOS

J. Singal[1], A. Kogut[2], E. Jones[1], and H. Dunlap[1]
[1] Physics Department, University of Richmond 28 Westhampton Way, Richmond, VA 23173, USA; jsingal@richmond.edu
[2] Code 665, NASA Goddard Space Flight Center Greenbelt, MD 20771, USA
Received 2014 August 28; accepted 2014 December 24; published 2015 January 19

ABSTRACT

We use surface brightness contour maps of nearby edge-on spiral galaxies to determine whether extended bright radio halos are common. In particular, we test a recent model of the spatial structure of the diffuse radio continuum by Subrahmanyan & Cowsik which posits that a substantial fraction of the observed high-latitude surface brightness originates from an extended Galactic halo of uniform emissivity. Measurements of the axial ratio of emission contours within a sample of normal spiral galaxies at 1500 MHz and below show no evidence for such a bright, extended radio halo. Either the Galaxy is atypical compared to nearby quiescent spirals or the bulk of the observed high-latitude emission does not originate from this type of extended halo.

Key words: Galaxy: halo – radio continuum: galaxies

CHANGES XII: N3556 (Miskolczi+, submitted)

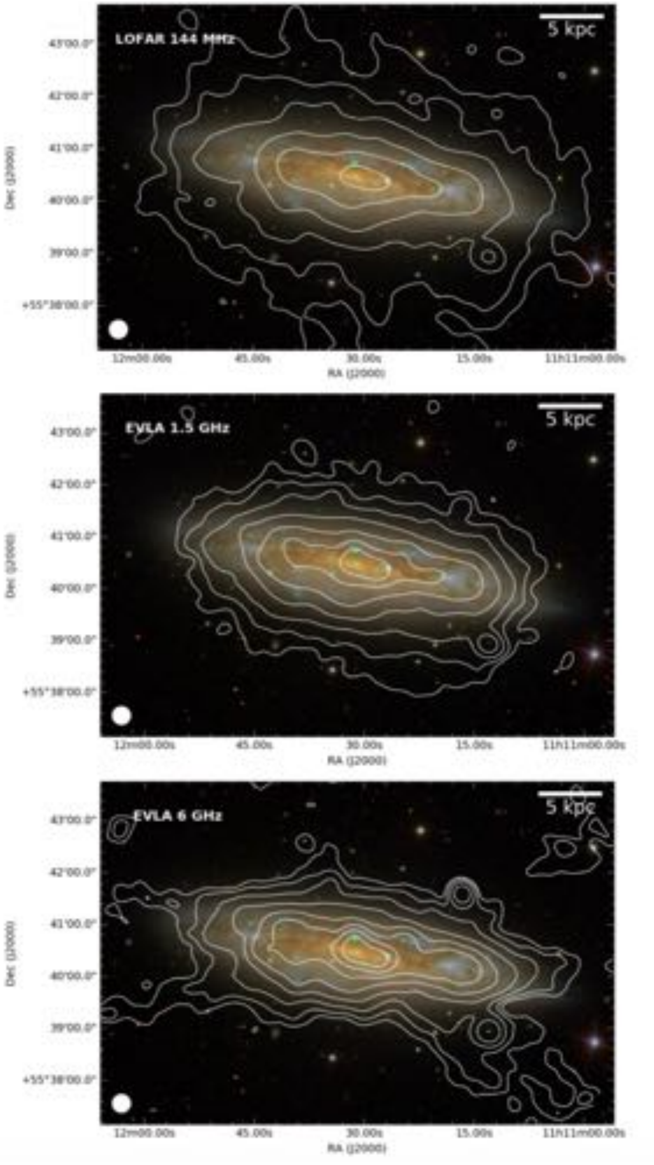

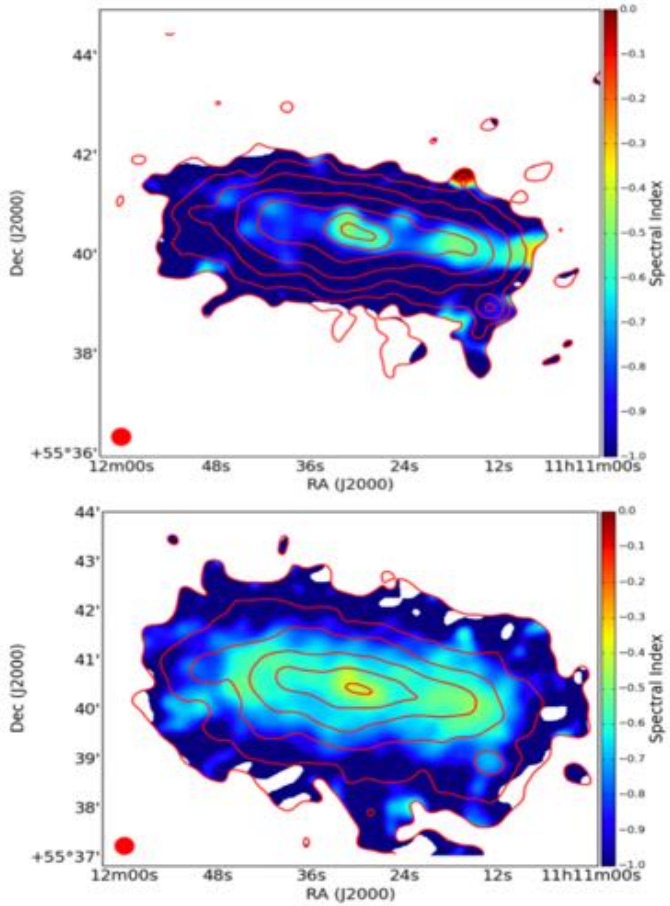

spectral index
much better
described using
a wind profile for v

$$v(z) = v_0 \left(1 + \left(\frac{z}{h_\mathrm{v}}\right)^{\beta}\right).$$

NGC 5775

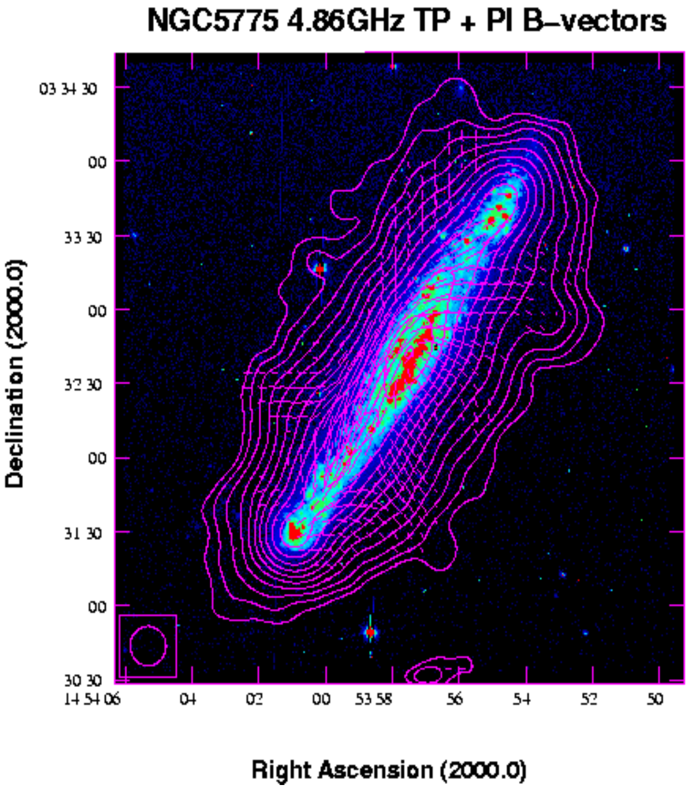

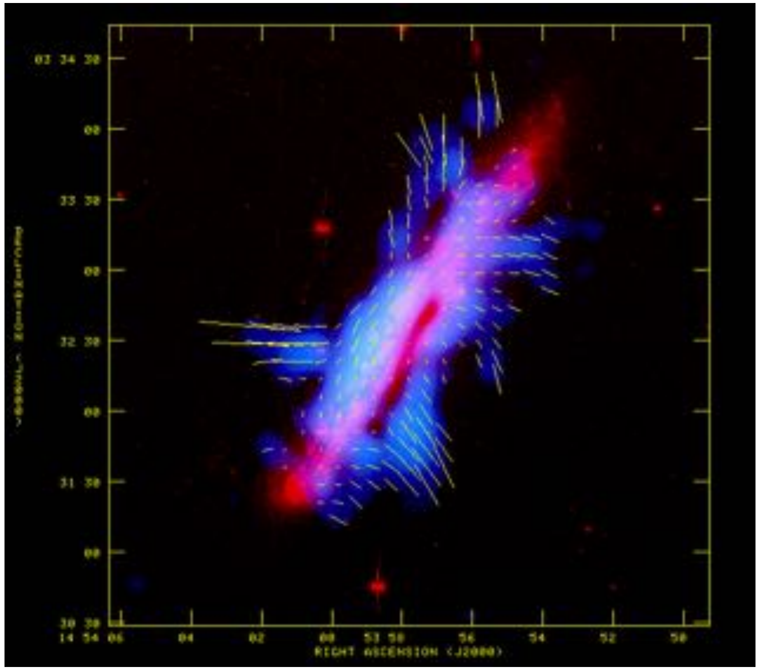

Soida, Krause, Dettmar, Urbanik A&A 2011
Tüllmann, Dettmar, Soida, et al. A&A, 2000 364,L36

LOFAR HBA 10hrs 118-192 MHz (Heald, Shridar, Heesen + LOFAR MKSP)

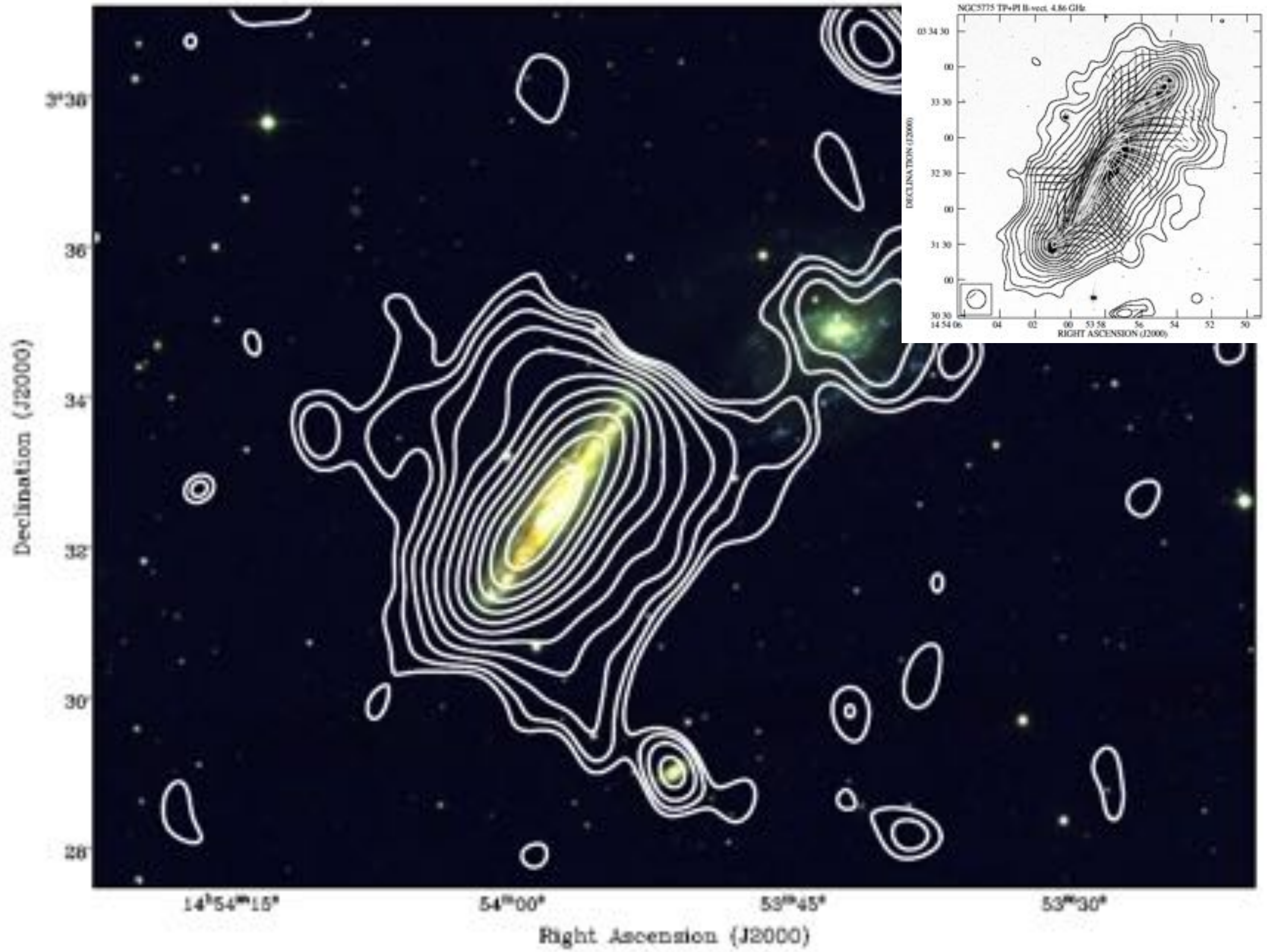

RUHR-UNIVERSITÄT BOCHUM

RUB

Summary:

- New broad-band multichannel receivers provide higher sensitivity and allow for new analysis techniques such as Rotation Measure Synthesis
- CRE transport seems to be dominated by advection in most star forming disk galaxies
- Halos of spiral galaxies have a significant magnetic field component, in star forming galaxies the x-shape structure in polarization is frequent
- RM distributions show large scale coherent B-field structures in halos

Supported by BMBF „Verbundforschung bodengebundene Astronomie und Astrophysik“

Thank you

NGC 46666 Credit: Y. Stein, J. Englisch, A. Miskolczi

Thank you

NGC 46666 Credit: Y. Stein, J. Englisch, A. Miskolczi